

ICEMG 2023-XXXXX

Torque Profile Enhancement of a Coaxial Transverse-Radial Flux Magnetic Gear Using Taguchi Optimization Method

Mahdi Abolghasemi¹, Aghil Ghaheri², Ebrahim Afjei³

¹Department of Electrical Engineering, Shahid Beheshti University, Tehran; m.abolghasemi@hotmail.com

²Department of Electrical Engineering, Shahid Beheshti University, Tehran; a_ghaheri@sbu.ac.ir

³Department of Electrical Engineering, Shahid Beheshti University, Tehran; e-afjei@sbu.ac.ir

Abstract

Torque and rotational speed scaling is a typical requirement of industry for a variety of applications. Magnetic gears benefit from numerous advantages due to their physically isolated rotors. Gearing action in magnetic gears occurs by the interaction of the modulated magnetic fields through modulators. The finite element method is typically utilized throughout the design process for magnetic devices. More than dozens of cases need be evaluated in the optimization procedure of a magnetic device to acquire the optimal size. Thus, it takes considerable time to obtain the optimal case. Taguchi method is originally a design of experiments method that drastically reduces number of experiments. This phenomenon is based on the reduction of output variation using orthogonal arrays. In this paper, a transverse-radial flux magnetic gear is optimized by Taguchi method. Signal-to-noise ratio and analysis of variance approaches are utilized to estimate the effective parameters, participation percentage, and optimal level for each control factor. Finally, a comparison is made between the optimal and initial designs, and it is shown that both the torque ripple and the maximum applicable torque have been improved by 40.03% and 30.83%, respectively.

Keywords: finite element method, magnetic gear, optimization, Taguchi method, transverse flux,

Introduction

In many industries, a high torque density has always been desired. The great torque and efficiency properties of transverse flux electrical machines are well-known in the scientific community [1]. Aerospace [2, 3], public transportation [4], hybrid vehicles, e-bikes [5], railway system [6], and etc. all make use of this electrical machine structure. Furthermore, torque density could be increased by attaching a mechanical gearbox to the rotating motor. Periodic maintenance, exhaustion and wear of teeth, periodic lubrication, high mechanical losses, high vibration and acoustic noise, teeth-crunching under overload condition, and so on are just a few of the many problems associated with mechanical gears. Their magnetic counterpart, however, is not affected by the aforementioned drawbacks [7].

In 1901, C. Armstrong was the one who came up with the concept of the magnetic gear (MG) for the first time [8]. In the years since, a few US patents have been filed on this matter to propose more structures for MGs due to the lack of high flux density magnets till 1980s [9-11]. K. Atallah et al. proved that coaxial radial MGs equipped with NdFeB rare-earth magnets can benefit from high torque density which makes MGs competitive

compared with their mechanical counterpart. Also, they have derived the relation between number of rotors pole pieces and modulators by analyzing air gaps magnetic flux distribution and its space harmonic spectrum in the vicinity of modulators inner and outer sides [12, 13]. Most research are focused on coaxial radial flux MGs, while transverse flux machines can transmit higher torque density if they have been designed with sufficient precision [14]. W. Bomela et al. have studied the performance of a transverse flux magnetic gear (TFMG) which its modulators transfer the flux in axial direction [15]. In [16], authors have proposed a TFMG with T-shaped modulators. They could reduce the leakage flux and soft magnetic material that improve the torque density. A coaxial axial-field-flux modulated is proposed in [17] that its modulators are placed in both sides surrounding all of the magnets. X. Li et al. have investigated the impact of fringing and end leakage fluxes on the torque characteristic of the TFMG [18]. M. B. Kouhshahi et al. have proposed an axial flux focusing magnetically geared generator which is integrated a generator and a TFMG to provide higher active volume torque for low input speed applications [19]. In [20], authors have studied the effect of back iron on the flux leakage and torque profile of a high performance MG. Two structure of MGs, segmented magnet and spoke type magnet, have been analyzed and it has been proved that the segmented magnet one is able to transfer 1.3 times higher torque than the conventional surface mounted structure [21]. B. Dai et al. have proposed an innovative technique for reduction of cogging torque of MGs. They announced and proved that the cogging torque would be diminished significantly by grouping each 3 modulators and optimizing the pole pitch of each modulator [22].

Finite element method (FEM) is the most known method for studying the magnetic devices behavior. The main defect of FEM is its time-consuming inherent feature. More than dozens of cases must be studied by FEM to optimize the dimension of a magnetic device. Taguchi method is a design of experiments method that lowers the number of cases with the help of orthogonal arrays. Generally speaking, it's a quality control method that diminishes the variations of output value [23]. B. Singh et al. have optimized a permanent magnet brushless DC (BLDC) motor utilized with Halbach array using the Taguchi method [24]. A multi-objective optimization has been applied on a BLDC motor with the aid of Taguchi method and signal-to-noise (S/N) ratios and analysis of variance (ANOVA) techniques [25]. Y. C. Wu et al. have optimized a coaxial radial flux magnetic gear by Taguchi method to enhance the transmitting torque [26].

In this paper a coaxial transverse-radial flux magnetic gear (TRFMG) has been proposed to be optimized, depicted in Figure 1. Magnets' layout of HSR and LSR are distinct in this embodiment. While the LSR magnets are of spoke type, the HSR ones are surface mounted. Taguchi method has been employed to optimize the structural parameters. By S/N ratios technique the severity and optimum level of each factor is obtained. Furthermore, the control factors' participation percentages have been derived by ANOVA technique and optimum levels obtained by S/N ratios are validated. At long last, evidence has accumulated showing that the Taguchi approach may successfully raise the maximum applicable torque per volume and lower the torque ripple.

Operating Principle

As MGs are considered as a passive magnetic device, no relation can be derived for their rated power. In order to design a MG, the worthiest parameter is its maximum applicable torque. The MG designer should focus on maximizing the transmitting torque that would lead to increasing the transmitting power of MG. Regarding to the MG sustainable rotational velocity, mechanical and thermal analysis must be applied and studied. In MGs, increasing the torque would not pursue the reduction of rotational velocity, necessarily. Determining the modulators and pole pairs counts is of most important designing procedure of MGs. These parameters can be obtained as follow [12]:

$$n_M = P_H + P_L \quad (1)$$

$$G_r = \frac{P_H - n_M}{P_H} = -\frac{P_L}{P_H} \quad (2)$$

Abovementioned equations are based on the magnetic flux density harmonic spectrum. In order to assay the validity of abovementioned relations, pole pairs count of the low speed rotor (LSR) would be obtained by harmonic spectrum analysis, while number of high speed rotor (HSR) and modulators are chosen. In this study, number of HSR pole pairs, modulators count, and gear ratio are assigned 4, 25, and 5.25, respectively.

In harmonic spectrum analysis, HSR would be rotated with 3000 rpm, while modulators are kept stationary. It must be mentioned that in this test there is no LSR as its pole pairs count is unclear. Figure 2 demonstrates the radial magnetic flux density distribution in adjacent to LSR due to the rotation of HSR. In addition, space harmonic spectrum of obtained radial magnetic flux density profile is depicted in Figure 3. It can be seen that the highest harmonic magnitude belongs to the 21th order. This means that the best choice for LSR pole pairs count is 21 to transmit higher torque density in accordance with mentioned HSR pole pairs and modulators counts. The exact Fourier transforms for 4th and 21st harmonic orders are shown in Figure 4 and Figure 5. It can be brightly observed that both curves are trying to conform their sinusoidal harmonic component. Similarly, in another test the HSR can be omitted, while LSR is rotated instead. Same results would be obtained in this case. The only difference is that the 4th harmonic order magnitude would gain the highest value as expected.

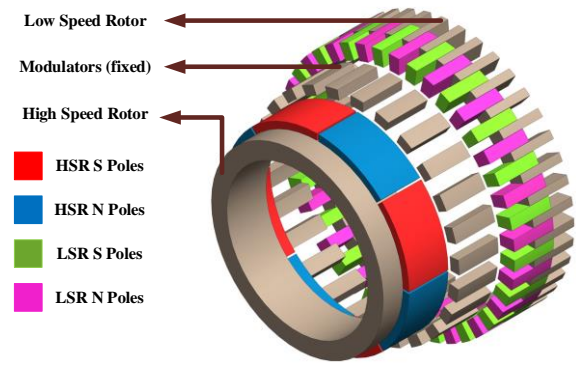


Figure 1. 3D exploded view of TRFMG

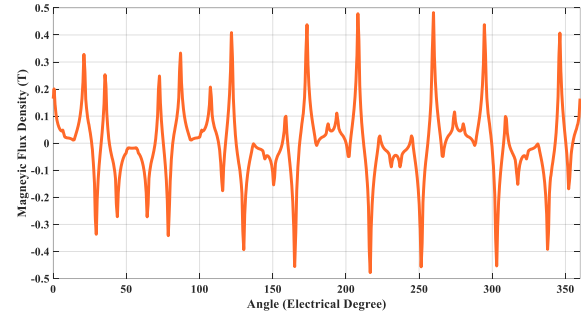


Figure 2. Radial magnetic flux density distribution when HSR is rotating, in the absence of LSR

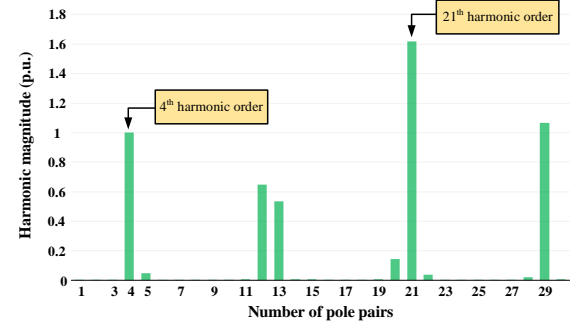


Figure 3. Space harmonic spectrum of radial magnetic flux density distribution when HSR is rotating

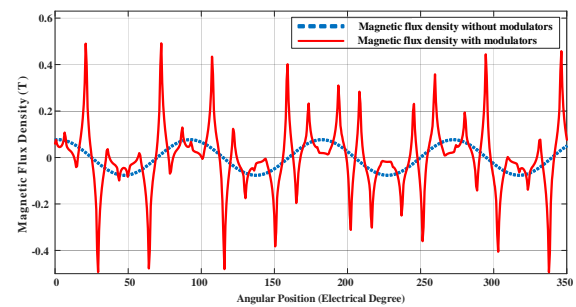


Figure 4. 4th component of radial magnetic flux density distribution when HSR is rotating, in the absence of LSR

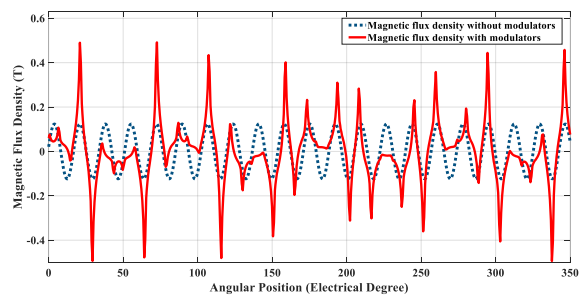


Figure 5. 21st component of radial magnetic flux density distribution when LSR is rotating, in the absence of HSR

Initial Design Discussion

The main goal of this study is optimizing a TRFMG using Taguchi method. The under study TRFMG contains of three main parts; LSR, HSR, and modulators. Magnets of HSR are of surface mounted type and there are 8 poles of them on the inner rotor. Outer rotor is utilized with spoke type magnets and magnetic flux passes through steel pieces to enter the air gap. Although, the arrangement of magnets on both rotors can be surface mounted or of spoke type but, Y. Chen et al. have proved in their research that the chosen structure in this study can provide a higher torque density [27]. Dimensions of initial design of under study TRFMG are given in Table 1. In order to study the behavior of any MG, two main test must be applied, blocked rotor and synchronous speed tests.

Blocked Rotor Test

One of the most important tests for MGs is blocked rotor test. In this test one of the rotors would be rotated with a specific rotational velocity while other rotor is kept stationary. Using the obtained results from this test, the maximum applicable torque would be derived. As it has been mentioned before, maximum applicable torque is a vital parameter in MGs. The maximum applicable torque of LSR and HSR are 59.31 and 11.36 (N.m),

respectively. It is noteworthy to mention that applying higher torques would lead to rotors slip. In this condition, rotors slip till the input torque lowers under the maximum applicable torque. This is one of the most unique features of MGs, the inevitable overload protection.

Synchronous Speed Test

Synchronous speed test is necessary to measure the severity of torque ripple and magnetic coupling validation. In this test, both rotors would be rotated in opposite directions with constant rotational speed. It must be considered that the initial design of each rotor is fixed in a way to achieve 40 (N.m) at LSR side. As modulators are sandwiched by LSR and HSR magnets, the main source of torque ripple in MGs is interaction between magnets and modulators. The higher the torque ripple, the higher vibration and acoustic noise would appear. The torque ripple and average torque of HSR and LSR are 0.82%, 7.62 (N.m), 5.89%, and 40 (N.m), respectively.

Optimization Procedure

As it has been mentioned before, Taguchi method is originally a design of experiments method. It uses orthogonal arrays to reduce number of required experiments. There are various structures of orthogonal arrays such as L4, L8, L9, and etc. It must be noted that all of the orthogonal arrays cannot be utilized for all combinations of control factors and levels. They are fully dependent on the number of control factors and their levels. Table 2 informs the mostly necessary orthogonal arrays with allowed control factors and levels counts.

For under study TRFMG, L27 orthogonal array has been adopted as 7 control factors with 3 levels have been chosen. This orthogonal array would decrease the number of required experiments from 2187 to 27. Assigned control factors are mainly structural parameters including LSR magnets pole pitch, HSR magnets pole pitch, modulators pole pitch, radial length of LSR magnets, radial length of HSR magnets, radial length of modulators, and LSR protrusion. These control factors are listed in Table 3. The L27 orthogonal array of under study MG is given in Table 4. Also, control factors are depicted in Figure 6. Obtained results from experiments can be analyzed using S/N ratios, analysis of mean (ANOM), and ANOVA techniques. In this study S/N ratios technique has been adopted to identify the optimum levels and severity of each factor. In addition, with the help of ANOVA, participation percentage of each control factor has be determined.

S/N Ratios Analysis

As S/N ratios technique benefit from 10-based logarithm transform of mean square deviation (MSD), it can suppress the variations of output, effectively. Its main relation is as follow:

$$S / N = -10 \log(MSD) \quad (3)$$

It is noteworthy to mention that three different objectives can be followed by S/N ratios. The larger is better, the nominal is better, and the smaller is better. So, MSD would be calculated in different way for each of them. MSD relations for each of the aforementioned objectives are given below.

The larger is better:

Table 1. Initial design structural parameters

Parameters	Values
Outer diameter of LSR	150 mm
Inner diameter of LSR	132 mm
Outer diameter of LSR magnets	150 mm
Inner diameter of HSR magnets	134 mm
Outer diameter of HSR	110 mm
Outer diameter of HSR magnets	118 mm
Inner diameter of HSR magnets	110 mm
Modulators outer diameter	131 mm
Modulators inner diameter	119 mm
Modulators pole pitch	50%
LSR magnets pole pitch	40%
HSR magnets pole pitch	90%
Air gap length	0.5 mm
Gear ratio	5.25

Table 2. Frequently used orthogonal arrays

Number of Levels	Orthogonal Array Type	Number of Factors
2	L4	2 and 3
	L8	2 to 7
	L12	2 to 11
	L16	2 to 15
	L32	2 to 31
3	L9	2 to 4
	L27	2 to 13
4	L16	2 to 5
5	L25	2 to 6
Mixed	L8	2 to 5
	L16	2 to 13
	L18	2 to 13
	L32	2 to 13
	L36	2 to 23
	L54	2 to 26

Table 3. Control factors, their levels and labels

Control Factors	Label	Level 1	Level 2	Level 3
LSR magnets pole pitch	A	0.4	0.5	0.6
HSR magnets pole pitch	B	0.9	0.95	1
Modulators pole pitch	C	0.5	0.55	0.6
Radial length of HSR magnets	D	4 mm	5 mm	6 mm
Radial length of LSR magnets	E	8 mm	10 mm	12 mm
Radial length of modulators	F	6 mm	8 mm	10 mm
LSR steel edge	G	1 mm	2 mm	3 mm

Table 4. L27 orthogonal array of TRFMG

Experiment No.	Levels Specification of Control Factors						
	A	B	C	D	E	F	G
1	1	1	1	1	1	1	1
2	1	2	1	1	1	2	2
3	1	3	1	1	1	3	3
4	2	1	2	1	2	1	1
5	2	2	2	1	2	2	2
6	2	3	2	1	2	3	3
7	3	1	3	1	3	1	1
8	3	2	3	1	3	2	2
9	3	3	3	1	3	3	3
10	1	2	2	2	3	3	1
11	1	3	2	2	3	1	2
12	1	1	2	2	3	2	3
13	2	2	3	2	1	3	1
14	2	3	3	2	1	1	2
15	2	1	3	2	1	2	3
16	3	2	1	2	2	3	1
17	3	3	1	2	2	1	2
18	3	1	1	2	2	2	3
19	1	3	3	3	2	2	1
20	1	1	3	3	2	3	2
21	1	2	3	3	2	1	3
22	2	3	1	3	3	2	1
23	2	1	1	3	3	3	2
24	2	2	1	3	3	1	3
25	3	3	2	3	1	2	1
26	3	1	2	3	1	3	2
27	3	2	2	3	1	1	3

$$MSD = \sum_{i=1}^n \frac{y_i^2}{n} \quad (4)$$

The nominal is better:

$$MSD = \sum_{i=1}^n \frac{(y_i - m)^2}{n} \quad (5)$$

The smaller is better:

$$MSD = \sum_{i=1}^n \frac{1}{y_i^2} \quad (6)$$

In this research, maximizing the maximum applicable torque per volume and minimizing the torque ripple are the main goals. As it is going to deal with a multi-objective optimization, it is necessary to normalize data properly and adopt one of the abovementioned MSD calculation relations. The larger is better is adopted for this work.

In order to avoid a pile of data, the optimization

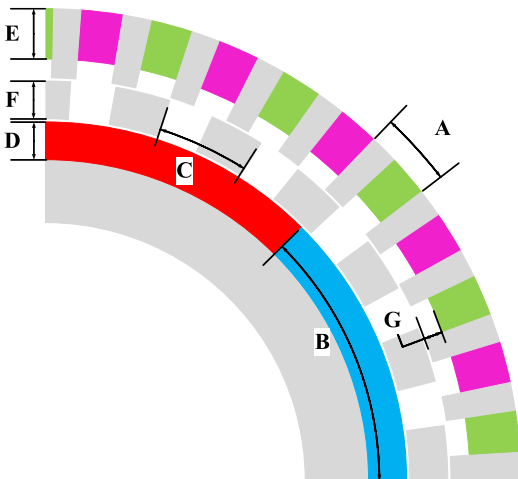


Figure 6. Control factors of TRFMG

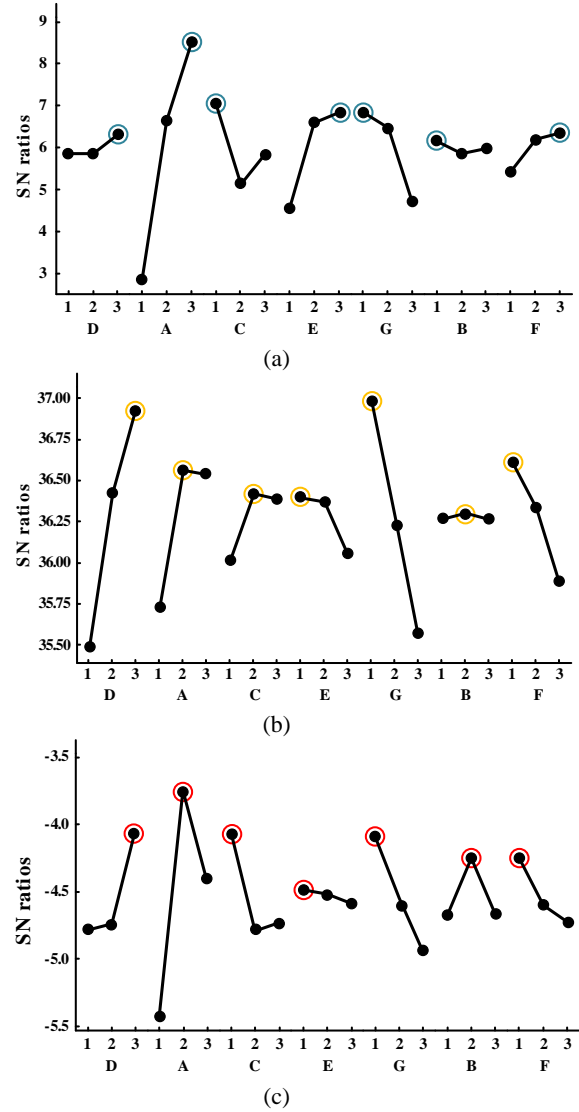


Figure 7. The S/N ratios of (a) LSR torque ripple (b) LSR maximum applicable torque per volume (c) Multi-objective function

procedure has been carried out by considering obtained results from LSR side. S/N ratios of control factors for torque ripple and maximum applicable torque per volume objectives are depicted in Figure 7 (a) and (b). It can be observed that the levels 3, 1, 1, 3, 3, 3, and 1 are the torque ripple optimum levels for LSR magnets pole pitch, HSR magnets pole pitch, modulators pole pitch, radial length of LSR magnets, radial length of HSR magnets, radial length of modulators, and LSR protrusion, respectively. while, levels 2, 2, 2, 3, 1, 1, and 1 are the optimum levels for maximum applicable torque per volume with the mentioned order. Also, it can be seen that the most effective control factors for torque ripple and maximum applicable torque per volume are LSR magnets pole pitch and radial length of HSR magnets, respectively.

For the purpose of multi-objective optimization, weighting equation has been utilized. In this method there is a weighting coefficient for each objective which defines its importance. This equation is written as follow:

$$MOOF = k_1 Max_{Norm} + k_2 Cog_{Norm} \quad (7)$$

Table 5. The ANOVA analysis obtained results for specified objectives

Factors	DOF	Maximum Applicable Torque / Vol.				Torque Ripple				Multi-Objective Function			
		SS	P(%)	F	P	SS	P(%)	F	P	SS	P(%)	F	P
A	2	224.66	15.13	28.25	2.9×10^{-5}	0.5544	63.85	34.77	1.02×10^{-5}	0.0659	32.35	5.13	0.025
B	2	2.39	0.16	0.3	0.746	0.0014	0.16	0.09	0.916	0.0072	3.53	0.62	0.556
C	2	49.17	3.31	6.18	0.014	0.0309	3.56	1.94	0.186	0.0163	8	1.27	0.316
D	2	509.53	34.31	64.08	3.9×10^{-7}	0.0082	0.94	0.52	0.608	0.0173	8.49	1.35	0.297
E	2	39.51	2.66	4.97	0.027	0.0864	9.95	5.42	0.021	0.0001	0.05	0.01	0.992
F	2	115.88	7.80	14.57	6.1×10^{-4}	0.0210	2.42	1.32	0.303	0.0078	3.83	0.61	0.562
G	2	496.06	33.41	62.38	4.6×10^{-7}	0.0701	8.07	4.39	0.037	0.0113	5.55	0.88	0.440
Error	14	47.71	3.21	-	-	0.0957	11.02	-	-	0.0771	37.84	-	-
Total	26	1484.91	100	-	-	0.8683	100	-	-	0.2037	100	-	-

In this study, k1 and k2 are assigned 0.7 and 0.3, respectively. S/N ratios of multi-objective analysis are depicted in Figure 7 (c). From this diagram it can be deduced that the optimum levels for mentioned control factors are 2, 2, 1, 3, 1, 1, and 1, respectively. It is evident from maintained data that the severity of control factors from the highest to the lowest are LSR magnets pole pitch, LSR protrusion, modulators pole pitch, radial length of HSR magnets, radial length of modulators, HSR magnets pole pitch, and radial length of LSR magnets, respectively.

ANOVA Analysis

As it has been mentioned, one of the main goals of ANOVA analysis is determining the exact participation percentage of each control factor. To achieve the reliable results, some parameters such as sum of squares (SS) of each factor, F-value, and P-value must be derived. There is a criterion in ANOVA analysis that distinguishes the effective control factors from others, known as P-value. The confidence percentage for this study has been assigned to 95% which means that control factors with P-value higher than 0.05 are not effective.

The ANOVA analysis results are given in Table 5.

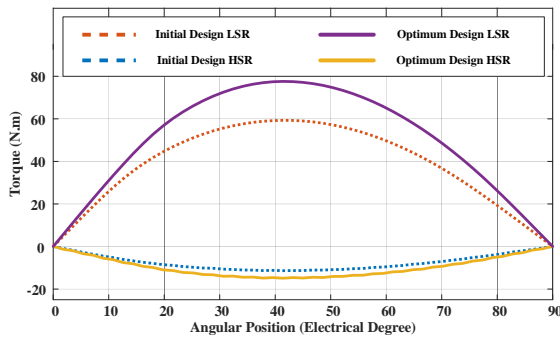


Figure 8. Blocked rotor test results of both initial and optimum designs

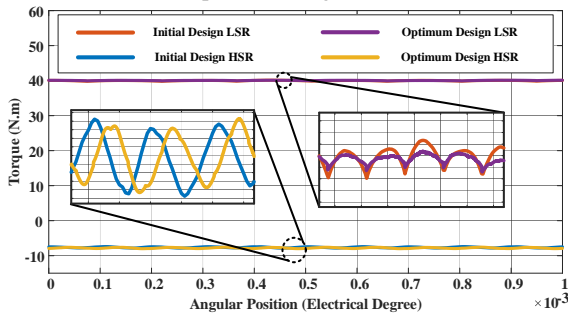


Figure 9. Torque comparison of both initial and optimum designs

Degree of freedom (DOF) of each control factor equals to 2. As the total DOF of whole system is 26, the error DOF would be 14. The total DOF has been derived by subtracting one from the total number of experiments. It can be seen from the multi-objective function section of Table 5 that LSR magnets pole pitch has the most significant effective factor. Furthermore, the participation percentage of LSR magnets pole pitch, HSR magnets pole pitch, modulators pole pitch, radial length of LSR magnets, radial length of HSR magnets, radial length of modulators, and LSR protrusion are 32.35%, 3.53%, 8%, 8.49%, 0.05%, 3.83%, and 5.55%, respectively. The error percentage of maximum applicable torque per volume, torque ripple, and multi-objective function are 3.21%, 11.02%, and 37.84%, respectively. The high error percentage of multi-objective function is due to interaction of control factors which has been ignored in this story.

Comparison of the initial and optimum cases

As it has been deduced from last sections, the optimum levels for control factors A to G are 2, 2, 1, 3, 1, 1, and 1, respectively. In initial design, first level has been assigned for all of the Control factors. From S/N ratios analysis it has been observed that LSR magnets pole pitch has the most effect on the LSR torque ripple, while radial length of HSR magnets is the most effective of maximum applicable torque per volume. All in all, in accordance with the assigned weighting coefficient, the LSR magnets pole pitch had the most significant effect on the multi-objective function. With a quick glance it can be observed that the set of optimum control factors' levels is not in the formed L27 orthogonal array of under study TRFMG. this proves and validates the optimum levels prediction ability of Taguchi method.

In Figure 8, the blocked rotor characteristics of both initial and optimum designs are shown. It can be seen that the maximum applicable torque of the under study TRFMG has been enhanced for 18.288 (N.m) or in other word 30.83%. In addition, results of synchronous speed test of the both designs are depicted in Figure 9. The torque ripple characteristic is improved slightly. Torque ripple of LSR side have been reduced to 0.466% which means 43.03% improvement. The magnetic flux distribution of optimum design is depicted in Figure 10.

Conclusion

In this paper, a TRFMG has been studied. The space harmonic spectrum of the proposed MG, while the HSR is rotating and LSR is stationary, has been provided. It has been observed that by a fixed number of HSR pole pairs and modulators count, number of LSR pole pairs

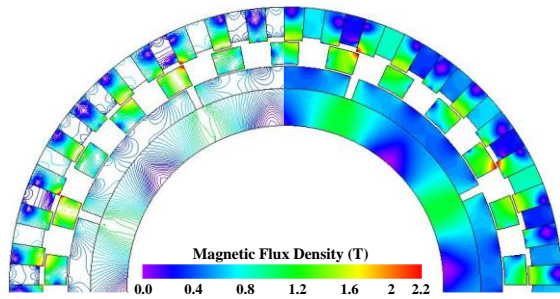


Figure 10. Magnetic flux Distribution of TRFMG optimum design

must be chosen equal to the highest value of obtained harmonic order. Seven control factors were adopted and labeled A to G with 3 levels for each of them. The Taguchi design of experiments method has been utilized to derive the optimum control factors' levels. As it has been noted in the corresponding section, the optimum level of control factors A to G are 2, 2, 1, 3, 1, 1, and 1, respectively. Also, the participation percentages of control factors with the same order are 32.35%, 3.53%, 8%, 8.49%, 0.05%, 3.83%, and 5.55%, respectively. LSR magnets pole pitch was the most effective control factor. Finally, by comparing the initial and optimum designs, it has been concluded that the maximum applicable torque and torque ripple of LSR side have enhanced for 18.288 (N.m) and 43.03%.

Nomenclatures

P_H	High speed rotor pole pair
P_L	Low speed rotor pole pair
n_M	Number of modulators
G_r	Gear ratio
k_1	Weighting coefficient of maximum applicable torque
k_2	Weighting coefficient of torque ripple
$MOOF$	Multi-objective optimization function

References

- [1] B. Kaiser, and N. Parspour, "Transverse Flux Machine-A Review," *IEEE Access*, vol. 10, pp. 18395-18419, 2022.
- [2] N. J. Baker, and S. Jordan, "Comparison of two transverse flux machines for an aerospace application," *IEEE Transactions on Industry Applications*, vol. 54, no. 6, pp. 5783-5790, 2018.
- [3] M. C. Kulan, N. J. Baker, and S. Turvey, "Manufacturing challenges of a modular transverse flux alternator for aerospace," *Energies*, vol. 13, no. 16, pp. 4275, 2020.
- [4] A. M. Elantably, A. "An approach to sizing high power density TFPM intended for hybrid bus electric propulsion," *Electric Machines & Power Systems*, vol. 28, no. 4, pp. 341-354, 2000.
- [5] C. Pompermaier, J. Washington, L. Sjöberg, and N. Ahmed, "Reduction of cogging torque in transverse flux machines by stator and rotor pole shaping," in *IEEE Energy Conversion Congress and Exposition (ECCE)*, 2016, pp. 1-7.
- [6] D. Kang, Y. Chun, and H. Weh, "Analysis and optimal design of transverse flux linear motor with PM excitation for railway traction," *IEEE Proceedings-Electric Power Applications*, vol. 150, no. 4, pp. 493-499, 2003.
- [7] A. Darabi, M. Abolghasemi, R. Mirzahassemi, and M. Sarvi-Maraghi, "Transient analysis of an axial flux magnetic gear," in *28th Iranian Conference on Electrical Engineering (ICEE)*, 2020, pp. 1-5.
- [8] C. G. Armstrong, "Power transmitting device," *US Pat. 6872922*, 1901.
- [9] A. Neuland, *Apparatus for transmitting power*, US Pat. 75616213, 1913.
- [10] H. Faus, *Magnet gearing*, US Pat. 2243555, 1941.
- [11] T. Martin Jr, *Magnetic transmission*, US Pat. 3378710, 1968.
- [12] K. Atallah, and D. Howe, "A novel high-performance magnetic gear," *IEEE Transactions on magnetics*, vol. 37, no. 4, pp. 2844-2846, 2001.

- [13] K. Atallah, S. Calverley, and D. Howe, "Design, analysis and realisation of a high-performance magnetic gear," *IEEE Proceedings-Electric Power Applications*, vol. 151, no. 2, pp. 135-143, 2004.
- [14] M. Chen, L. Huang, Y. Li, P. Tan, G. Ahmad, Y. Liu, and M. Hu, "Analysis of Magnetic Gearing Effect in Field-Modulated Transverse Flux Linear Generator for Direct Drive Wave Energy Conversion," *IEEE Transactions on Magnetism*, vol. 58, no. 2, pp. 1-5, 2021.
- [15] W. Bomela, J. Z. Bird, and V. M. Acharya, "The performance of a transverse flux magnetic gear," *IEEE transactions on magnetics*, vol. 50, no. 1, pp. 1-4, 2013.
- [16] X. Yin, P.-D. Pfister, and Y. Fang, "A novel magnetic gear: toward a higher torque density," *IEEE Transactions on Magnetism*, vol. 51, no. 11, pp. 1-4, 2015.
- [17] D. Zhu, F. Yang, Y. Du, F. Xiao, and Z. Ling, "An axial-field flux-modulated magnetic gear," *IEEE Transactions on Applied Superconductivity*, vol. 26, no. 4, pp. 1-5, 2016.
- [18] X. Li, S. Liu, Y. Wang, and Y. Fan, "Investigation of the flux leakage effects in transverse-flux magnetic gear," in *20th International Conference on Electrical Machines and Systems (ICEMS)*, 2017, pp. 1-5.
- [19] M. B. Kouhshahi, J. Z. Bird, V. M. Acharya, K. Li, M. Calvin, W. Williams, and S. Modaresahmadi, "An axial flux focusing magnetically geared generator for low input speed applications," *IEEE Transactions on Industry Applications*, vol. 56, no. 1, pp. 138-147, 2019.
- [20] C. Tan, and L. Jing, "A Novel High Performance Magnetic Gear with Auxiliary Silicon Steel Sheet," *CES Transactions on Electrical Machines and Systems*, vol. 6, no. 2, pp. 201-206, 2022.
- [21] B. Dai, K. Nakamura, Y. Suzuki, Y. Tachiya, and K. Kuritani, "Comparison of Two Different Interior Permanent Magnet Type Low-speed Rotor Structures of Axial-Flux Magnetic Gear," *IEEE Journal of Industry Applications*, vol. 10, no. 6, pp. 632-637, 2021.
- [22] B. Dai, K. Nakamura, Y. Suzuki, Y. Tachiya, and K. Kuritani, "Cogging Torque Reduction of Integer Gear Ratio Axial-flux Magnetic Gear for Wind-Power Generation Application by Using Two New Types of Pole-Pieces," *IEEE Transactions on Magnetism*, vol. 58, no. 8, pp. 1-5, 2022.
- [23] W. Zhu, X. Yang, and Z. Lan, "Structure optimization design of high-speed bldc motor using Taguchi method," in *International Conference on Electrical and Control Engineering*, 2010, pp. 4247-4249.
- [24] B. Singh, S. Shastri, and U. Sharma, "Robust Design of a Ceiling Fan Halbach Array PMBLDC Motor using Taguchi Orthogonal Array," in *IEEE International Conference on Computing, Power and Communication Technologies (GUCON)*, 2020, pp. 430-435.
- [25] A. M. Ajamloo, A. Ghaheri, and E. Afjei, "Multi-objective optimization of an outer rotor BLDC motor based on Taguchi method for propulsion applications," in *10th International Power Electronics, Drive Systems and Technologies Conference (PEDSTC)*, 2019, pp. 34-39.
- [26] Y.-C. Wu, M.-C. Tsai, S. N. Fajri, and F.-M. Ou, "Design of coaxial magnetic gear mechanisms using Taguchi method," in *3rd IEEE International Conference on Knowledge Innovation and Invention (ICKII)*, 2020, pp. 1-5.
- [27] Y. Chen, W. N. Fu, S. L. Ho, and H. Liu, "A quantitative comparison analysis of radial-flux, transverse-flux, and axial-flux magnetic gears," *IEEE Transactions on Magnetism*, vol. 50, no. 11, pp. 1-4, 2014.